

Reactions of Nitrosoalkenes with Dipyrromethanes and Pyrroles: Insight into the Mechanistic Pathway

Sandra C. C. Nunes,[†] Susana M. M. Lopes,[†] Clara S. B. Gomes,[‡] Américo Lemos,[§] Alberto A. C. C. Pais,[†] and Teresa M. V. D. Pinho e Melo^{*†}

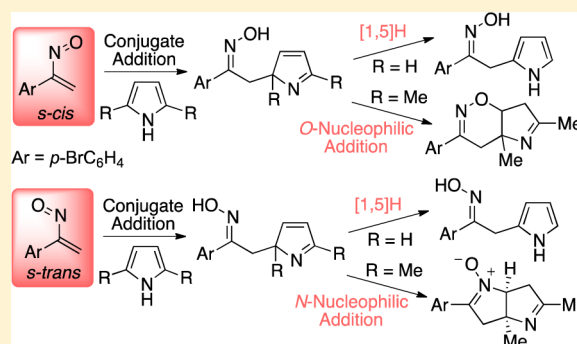
[†]Department of Chemistry, University of Coimbra, 3004-535 Coimbra, Portugal

[‡]Centro de Química Estrutural, Departamento de Engenharia Química, Instituto Superior Técnico, University of Lisbon, 1049-001 Lisboa, Portugal

[§]CIQA, FCT, University of Algarve, Campus de Gambelas, 8005-139 Faro, Portugal

Supporting Information

ABSTRACT: The reactivity of nitrosoalkenes toward dipyrromethanes, pyrrole, and 2,5-dimethylpyrrole is described. 1-(*p*-Bromophenyl)nitrosoethylene shows a different chemical behavior with these heterocycles than the previously reported reactions of ethyl nitrosoacrylate, which proceeds via a Diels–Alder reaction. 1-(*p*-Bromophenyl)nitrosoethylene reacts with dipyrromethanes and pyrrole to afford two isomeric oximes via conjugate addition followed by rearomatization of the pyrrole unit. On the other hand, this nitrosoalkene reacts with 2,5-dimethylpyrrole through an initial conjugate addition followed by intramolecular O- and N-nucleophilic addition with the formation of the corresponding bicyclic oxazine and five-membered cyclic nitron, respectively. Quantum chemical calculations, at the DFT level of theory, indicate that the barriers associated with the Diels–Alder reactions of ethyl nitrosoacrylate are over 30 kJ/mol lower than those that would be required for the cycloadditions of 1-(*p*-bromophenyl)nitrosoethylene. Thus, calculations predict that the Diels–Alder reaction is privileged in the case of ethyl nitrosoacrylate and point to a different reaction pathway for 1-(*p*-bromophenyl)nitrosoethylene, corroborating the experimental findings.



INTRODUCTION

The reaction of nitrosoalkenes with pyrrole can be used as an approach to promote alkylation at the 2-position, leading to derivatives containing open-chain oximes. In fact, pyrrole reacts with conjugated nitrosoalkenes **2**, generated in situ by base-mediated dehydrobromination of α -halooximes **1**, to give pyrroles **4**. The formation of these products can be rationalized by considering the rearomatization of the initially formed Diels–Alder cycloadducts, bicyclic 1,2-oxazines. Oximes **4** were isolated as single stereoisomers, which were assigned as *anti* isomers, the expected outcome for the ring-opening reaction of bicyclic 1,2-oxazines. Evidence for the generation of the nitrosoalkenes **2** followed by Diels–Alder reaction also comes from the reaction of α -halooximes **1** with 2,5-dimethylpyrrole. In this case, the initially formed cycloadducts tautomerize to the corresponding 5,6-dihydro-4*H*-1,2-oxazines **5** (Scheme 1).^{1,2}

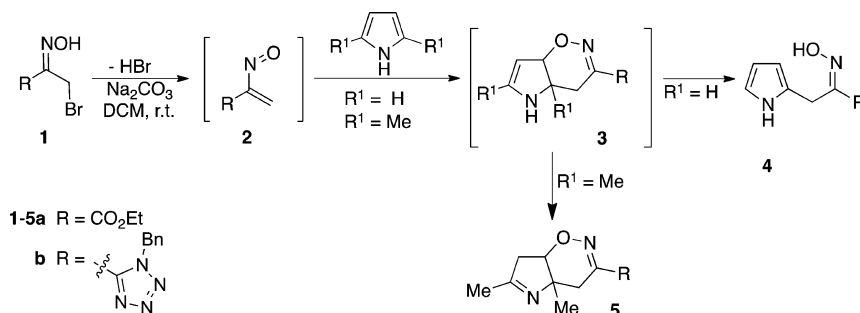
Moreover, the reaction of conjugated nitrosoalkenes with olefins has been explored as a general route to oxazines, the expected Diels–Alder cycloadducts.³ It is generally accepted that Diels–Alder cycloadditions between asymmetrically substituted dienes or heterodienes and/or asymmetrically substituted dienophiles take place through highly asymmetric transition state structures. These reactions are characterized by

an asynchronous bond formation, a process initiated by the formation of the first σ -bond between the most electrophilic and nucleophilic centers of the reagents with concomitant ring-closure. Domingo et al. have carried out quantum chemical calculations to study an extreme case of a polar Diels–Alder reaction, the reaction of nitrosoalkenes (electrophilic heterodienes) with enamines, which are among the most nucleophilic dienophiles.⁴ The results were in agreement with a two-stage, one-step mechanism, with C–C bond formation taking place in the first stage and the subsequent ring closure with the formation of the C–O bond taking place in the second stage.

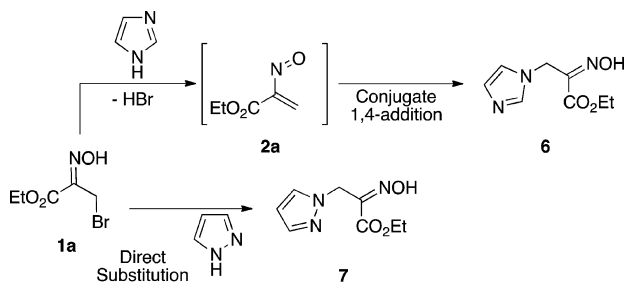
Reaction of nucleophiles with α -halooximes can involve two different mechanistic pathways: generation of nitrosoalkenes followed by conjugate 1,4-addition or direct substitution of the halogen. However, the intermediacy of nitrosoalkenes has been demonstrated by spectroscopic studies and in some cases by the direct isolation of more stable nitrosoalkenes.³ On the other hand, Gilchrist et al. have shown that ethyl bromopyruvate oxime (**1a**) reacts with imidazole faster than with the corresponding O-alkylated oxime, for which dehydrobromina-

Received: September 10, 2014

Published: October 13, 2014

Scheme 1. Reaction of Ethyl 2-Nitrosoacrylate and 1-Benzyl-5-(1-nitrosovinyl)-1*H*-terazole with Pyrrole Derivatives^{1,2}

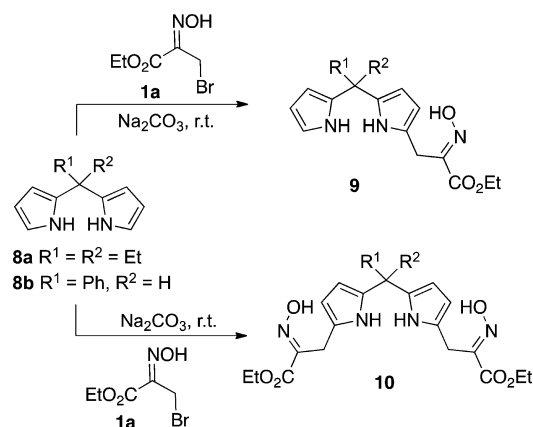
tion is precluded.⁵ This result indicates that ethyl bromopyruvate oxime reacts with imidazole by an elimination–addition mechanism, whereas the O-alkylated oxime undergoes direct substitution. In fact, imidazole was shown to be a strong enough base to eliminate HBr from **1a**, generating ethyl 2-nitrosoacrylate. It was also demonstrated that less basic azoles (e.g., pyrazole) react by direct displacement (Scheme 2).⁵

Scheme 2. Reaction of Ethyl 2-Nitrosoacrylate with Azoles⁵

The alkylation of pyrrole via reaction with α -halooximes is carried out in the presence of a base to ensure the generation of nitrosoalkenes. However, there is always the question of whether a hetero-Diels–Alder reaction or a conjugate 1,4-addition is taking place. Although the experimental evidence available so far indicates that Diels–Alder cycloadditions are involved, this is still a topic of debate.

This chemistry was explored as a new strategy for the functionalization of dipyrrmethanes, a class of compounds of wide interest as building blocks of porphyrinoids as well as BODIPY dyes (4,4-difluoro-4-bora-3a,4a-diaza-*s*-indacenes), which are also finding application as photonic organic-based materials and as optical anion sensors.⁶ We reported that 5,5'-diethyl- and 5-phenyldipyrrmethanes (**8**) participate in hetero-Diels–Alder reactions with nitrosoalkenes and azoalkenes to give dipyrrmethanes with side chains containing oxime and hydrazone groups, respectively, at positions 1 and 9.⁷ By controlling the reaction stoichiometry, it is possible to get mono or 1,9-disubstituted derivatives. The study included the reaction with ethyl 2-nitrosoacrylate leading to functionalized derivatives **9** and **10** as single stereoisomers (Scheme 3). More recently, we described a novel one-pot route to 5-substituted dipyrrmethanes by an on-water bis-hetero-Diels–Alder reaction of azo- and nitrosoalkenes with pyrrole.⁸

As part of our continuing investigations, we set out to further explore the methodology for the functionalization of dipyrrmethanes based on the hetero-Diels–Alder reaction of nitrosoalkenes, including 1-(1*H*-tetrazol-5-yl)nitrosoethylene derivatives. The results thus obtained led to a more detailed

Scheme 3. Functionalization of Dipyrrmethanes via Hetero-Diels–Alder Reactions of Ethyl 2-Nitrosoacrylate (**2a**)⁷

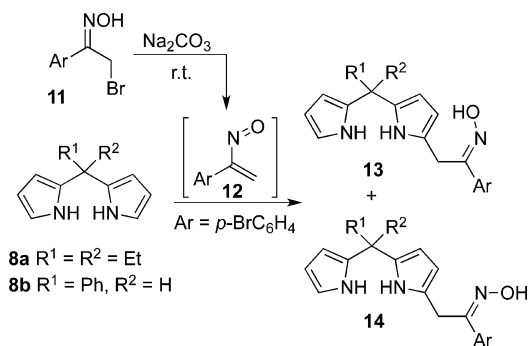
mechanistic study. Quantum chemical calculations were carried out, at the DFT level of theory, in order to rationalize the observed reactivity.

RESULTS AND DISCUSSION

The reaction of nitrosoalkene **12**, generated in situ from the corresponding bromooxime **11**, with dipyrrmethanes **8** was studied (Table 1). Initially, reactions were carried out at room temperature in dichloromethane using sodium carbonate as base, the reaction conditions previously described for the [4 + 2] cycloaddition of ethyl nitrosoacrylate with dipyrrmethanes⁷ (entries 1 and 3). Two equivalents of the dipyrrmethane were used in order to ensure the monofunctionalization. Unexpectedly, two isomeric oximes were obtained. Starting from 5,5'-diethyldipyrrmethane (**8a**), oximes **13a** and **14a** were isolated in 46 and 36% yields, respectively, whereas the reaction of 5-phenyldipyrrmethane (**8b**) gave oxime **13b** in 26% yield and oxime **14b** in 37% yield.

It has been shown that the reaction of azoalkenes with dipyrrmethanes using the solvent system water/dichloromethane as the reaction media instead of dichloromethane leads to higher yields with shorter reaction times.^{7b} Thus, the reaction of 1-(*p*-bromophenyl)nitrosoethylene (**12**) with dipyrrmethanes **8** was carried out under these reaction conditions (entries 2 and 4). In fact, shorter reaction times were required, although lower overall yields were obtained.

The molecular structure of (*E*)-1-(2'-*p*-bromophenyl-2'-hydroxyiminoethyl)-5,5'-diethyldipyrrmethane (**13a**) was established by X-ray crystallography (see Supporting Information). This compound crystallized as colorless plates in the triclinic system within the *P*-1 space group, showing two

Table 1. Reaction of Nitrosoalkene 12 with Dipyrrromethanes 8

entry	dipyrrromethane	conditions	13/14 ^a	isolated yields	
1	8a	DCM, 44 h	60:40	13a , 46%	14a , 36%
2	8a	H ₂ O/DCM (9:1.5 mL), 2 h	40:60	13a , 16%	14a , 27%
3	8b	DCM, 24 h	40:60	13b , 26%	14b , 37%
4	8b	H ₂ O/DCM (9:1.5 mL), 2 h	27:73	13b , 13%	14b , 27%

^aRatio of the crude mixture determined by ¹H NMR spectroscopy.

independent molecules per asymmetric unit. In one of these molecules (molecule A), the atom C15 shows a certain extent of disorder over two positions, with probabilities of 53 and 47%. The hydroxyl group of the oxime points toward the pyrrole moiety. This fact is attested by the shortest distance observed between the OH and the pyrrole [4.546 Å (molecule A) and 4.499 Å (molecule B)] when compared to the that displayed by the *p*-bromophenyl moiety [distances of 5.465 and 5.468 Å for molecules A and B, respectively]. The dihedral angles between these groups are pyrrole and C=N–OH, 80.0(3)° and 62.8(3)°; *p*-bromophenyl and C=N–OH, 24.0(3)° and 17.5(3)°; and *p*-bromophenyl and pyrrole, 85.5(3)° and 54.4(3)° for molecules A and B, respectively. All distances and angles are within the expected values for similar compounds.⁹ At a supramolecular level, it is possible to observe the existence of four hydrogen bonds, consistent with the distances (1) O(19A)–H(19A)⋯N(18A) of 2.07 Å [O(19A)⋯N(18A), 2.796(5) Å; O(19A)–H(19A)⋯N(18A), 144°; symmetry operation: 1 – *x*, –1 – *y*, 1 – *z*]; (2) N(10B)–H(100)⋯O(19A) of 2.45(5) Å [N(10B)⋯O(19A), 2.990(6) Å; N(10B)–H(100)⋯O(19A), 120(4)°]; (3) N(11A)–H(111)⋯N(18B) of 2.20(3) Å [N(11A)⋯N(18B), 3.064(6) Å; N(11A)–H(111)⋯N(18B), 164(5)°]; and (4) N(11B)–H(112)⋯O(19B) of 2.18(3) Å [N(11B)⋯O(19B), 2.883(5) Å; N(11B)–H(112)⋯O(19B), 139(4)°].

This allowed us to establish that the oxime group of dipyrrromethane **13a** has an *E* configuration. The configuration in the other derivatives was established by comparison of the ¹H NMR spectra.

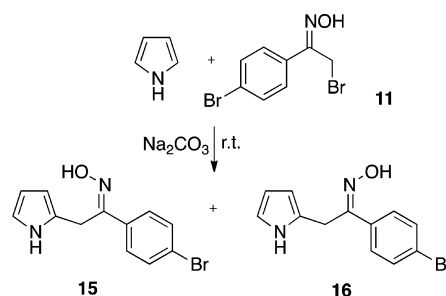
The outcome of the reaction of dipyrrromethanes **8** with nitrosoalkene **12** was unexpected. In fact, from a hetero-Diels–Alder reaction, the formation of the corresponding 1,2-oxazine was expected followed by ring-opening, leading to the selective synthesis of oximes **13**. However, two isomeric oximes were obtained, indicating that conjugate 1,4-addition may be the mechanistic pathway or a competitive process.

This result also shows that the replacement of the ester group of ethyl 2-nitrosoacrylate by an aryl group leads to a

different chemical behavior of the reactive intermediate toward dipyrrromethanes. The reaction with azoalkene **2a** affords single stereoisomers, whereas with *p*-bromophenyl derivative **12** isomeric oximes are obtained.

We decided to study the reactivity of pyrrole and 2,5-dimethylpyrrole toward nitrosoalkene **12**, which could be used as a model reaction for a more detailed mechanistic study. In fact, the comparison of these reactions with the known cycloaddition of pyrrole and 2,5-dimethylpyrrole with ethyl nitrosoacrylate (Scheme 1) could give new insight into the conjugated nitrosoalkene chemistry.

Interestingly, dehydrobromination of α -bromooxime **11** in the presence of pyrrole afforded the isomeric oximes **15** and **16** when carrying out the reaction in dichloromethane or in water/dichloromethane (Table 2). When using dichloromethane as

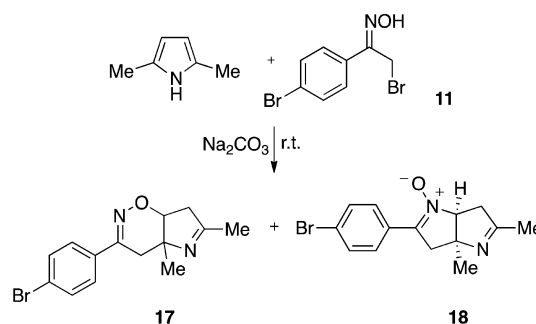
Table 2. Reaction of Nitrosoalkene 12 with Pyrrole

entry	conditions	15/16 ^a	isolated yields	
1	DCM, 40 h	72:28	15 , 37%	16 , 15%
2	H ₂ O/DCM (9:1.5 mL), 2 h	39:61	15 , 28%	16 , 44%

^aRatio of the crude mixture determined by ¹H NMR spectroscopy.

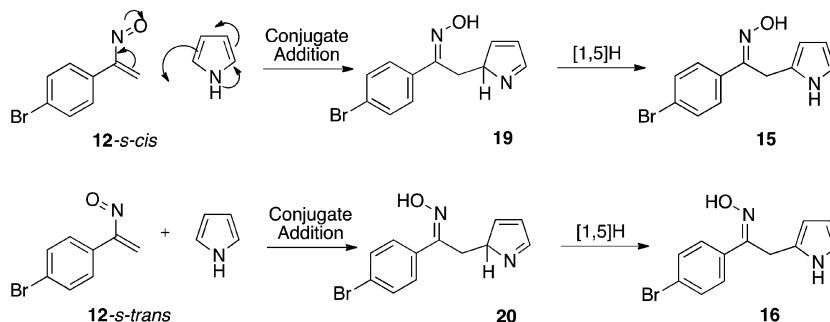
solvent, the mixture of oximes **15/16** (72:28 ratio) is formed in 52% overall yield. When carrying out the reaction in water/dichloromethane, oximes were isolated in higher overall yield (72%), with oxime **16** being the major product.

2,5-Dimethylpyrrole reacted with nitrosoalkene **12**, generated in situ from oxime **11**, to afford two products (Table 3). When carrying out the reaction at room temperature in dichloromethane, bicyclic oxazine **17** was isolated in 43% yield together with the synthesis of nitron **18** in 31% yield (entry 1). The same products were obtained in 78% overall yield by performing the reaction in water/dichloromethane, although

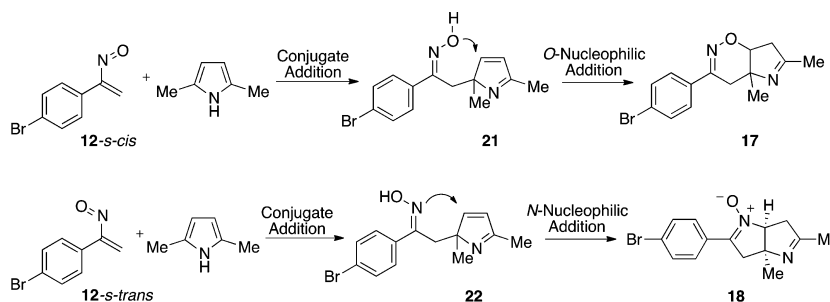
Table 3. Reaction of Nitrosoalkene 12 with 2,5-Dimethylpyrrole

entry	conditions	isolated yields	
1	DCM, 6 h	17 , 43%	18 , 31%
2	H ₂ O/DCM (9:1.5 mL), 2 h	17 , 30%	18 , 48%

Scheme 4. Mechanism Proposal for the Synthesis of Oximes 15 and 16



Scheme 5. Mechanism Proposal for the Synthesis of Bicyclic Oxazine 17 and Nitron 18



under these reaction conditions, nitron **18** (48%) was the major product (entry 2).

The molecular structure of derivative **18** was established unambiguously by X-ray crystallography (see Supporting Information). This compound crystallized as colorless irregular plates in the monoclinic system within the $P2_1/n$ space group, showing one independent molecule per asymmetric unit. Its molecular structure shows an *endo* conformation composed of two fused heterocyclic five-membered rings. The substituents at the C3A and C6A positions, a methyl group (C8) and a hydrogen, respectively, are *cis*, i.e., they are placed on the same faces of the fused rings. All distances and angles are within the expected values for similar compounds.⁹

The results on the reactivity of nitrosoalkene **12** toward pyrrole and 2,5-dimethylpyrrole are not consistent with a process involving hetero-Diels–Alder reactions. In fact, the reaction of pyrrole with nitrosoalkene **12** through a conjugate addition followed by rearomatization of the pyrrole would lead to two isomeric oximes, as observed experimentally. Starting from nitrosoalkene **12** at the *s-cis* conformation, oxime **15** is obtained, whereas *12-s-trans* affords oxime **16** (Scheme 4).

The reaction of 2,5-dimethylpyrrole can also be explained by considering an initial conjugate addition. However, since the rearomatization of the pyrrole ring is precluded, alternative pathways led to the final products. The addition of 2,5-dimethylpyrrole to *12-s-cis* gives intermediate **21** followed by intramolecular O-nucleophilic addition with the construction of the oxazine ring. On the other hand, 2,5-dimethylpyrrole adds to *12-s-trans* to give intermediate **22**, which undergoes cyclization via N-nucleophilic addition to the C–C double bond with the formation of the five-membered cyclic nitron **18** (Scheme 5). Support for this mechanistic proposal comes from the known cyclization of γ -functionalized oximes. Oximes bearing an electrophilic center at the γ -position undergo cyclization through nucleophilic substitution or nucleophilic addition reactions and can lead not only to oxazines but also to cyclic nitrones.^{10,11} Intermediates **21** and **22** have this structural

feature, and since the oximino group can act as both an O- and N-nucleophile, oxazines **17** and nitron **18** can be formed. Moreover, it has been reported that α -nitrosostyrenes react with 2-methoxypropene, leading to the corresponding oxazines together with the formation of five-membered cyclic nitrones.^{3d,11}

It is noteworthy that the observed ratio of oximes **15/16** is similar to the ratio obtained for compounds **17/18**. This observation is in agreement with the proposed mechanism since compounds **15** and **17** were derived from nitrosoalkene *12-s-cis* and compounds **16** and **18** were derived from *12-s-trans*.

The above-described results indicate that nitrosoacrylate (**2a**) reacts with pyrrole, 2,5-dimethylpyrrole, and dipyrromethanes via a Diels–Alder reaction, but a different reactivity was observed in the reaction of these heterocycles with 1-(*p*-bromophenyl)nitrosoethylene (**12**).

Therefore, quantum chemical calculations were carried out in order to investigate the reactivity of pyrrole and 2,5-dimethylpyrrole toward ethyl nitrosoacrylate (**2a**) and nitrosoalkene **12** (see Supporting Information). Calculations were performed by combining the capabilities of Gaussian 03¹² and Gamess¹³ program packages. The former was used for dihedral scans, and the latter, for geometry optimizations and frequency calculations. Graphical representations were produced with Gaussview and Molden 5.0.

Toward this end, the structure and the preferred conformations of molecules **2a** and **12** were investigated. In this context, preliminary relaxed potential energy surface scans (PES) around the dihedrals considered to be more relevant in each molecule were performed at the semiempirical PM3 level. The selected dihedrals for molecules **2a** and **12** indicated in Figure 1 were stepped using step sizes of 30° and 20°, respectively. The obtained scans are represented in Figure 2, in which, for convenience, is also included the contour profiles that help in the identification of the respective minima. For both molecules, the resulting PESs show a highly flat surfaces

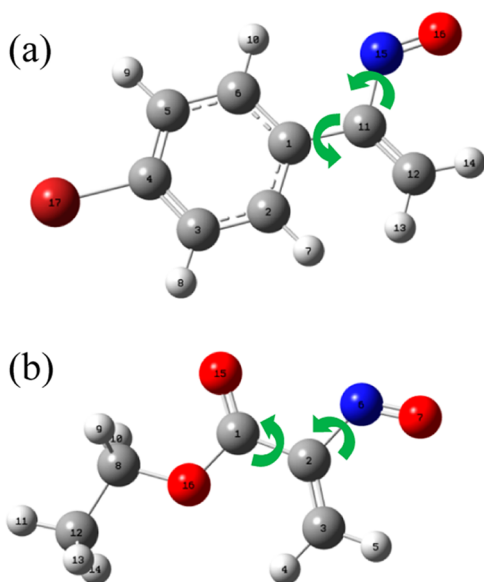


Figure 1. Geometries of nitrosoalkenes **12** (a) and **2a** (b) with the scanned dihedrals indicated. Color code: gray, carbon; red, oxygen; blue, nitrogen; white, hydrogen; and dark red, bromide.

with a wide range of possible orientations for the considered dihedrals within a very low energy range (below 12 kJ/mol). In each case, the identified absolute minima were fully optimized at the DFT level of theory using the B3LYP hybrid functional¹⁴ and the standard 6-31G(d,p) basis set. For compound **12**, full optimization produced two isoenergetic mirror image conformers, **c12a** and **c12b**, characterized by ϕ (C6–C1–C11–N15) = -22° and 22° , respectively, and ϕ (C1–C11–N15–O16) = -165° and 165° , for **c12a** and **c12b**, respectively. In the case of compound **2a**, the refinement at the DFT level also resulted in two isoenergetic conformers, **c2a1** and **c2a2** with ϕ (N6–C2–C1–O15) = -178° and 177° , respectively, and ϕ (O7–N6–C2–C1) = -164° for **c2a1** and 165° for **c2a2**. The final structures resulting from the DFT optimization are depicted in Figure 3. Moreover, the results expressed both in Schemes 4 and 5 and in Tables 2 and 3 prompted us to additionally explore the stability of the **12-s-trans** and **2a-trans** conformations at the DFT level. The highly flat PES indicates that a wide number of conformations are possible in a low energy range. In fact, the refinement of these two *trans* conformations gave rise to the conformers that are also included in Figure 4, which were characterized by an energy difference of $E_{cis} - E_{trans} = -0.4$ kJ/mol for **2a** and $E_{cis} - E_{trans} = 5.6$ kJ/mol for nitrosoalkene **12** and an increase in the electrostatic moment from **12-cis** (2.16D) to **12-trans** (2.80D) and from **2a-cis** (1.32D) to **2a-trans** (1.86D). These results are in accordance with the data presented in Tables 2 and 3 that suggest a preference for the *trans* conformer in more polar medium (H₂O/DCM).

In this study, transition states resulting from the *endo*- and *exo*-cycloadditions of pyrrole and dimethylpyrrole, also optimized at the DFT level, with nitrosoalkenes **2a** and **12** were considered. In each case, full geometry optimizations of the transition structures were performed at the B3LYP/6-31G(d,p) level, followed by harmonic frequency calculations at the same level of theory, which confirmed the nature of the stationary points. The starting structure in each case was derived from the *cis* conformers, depicted in Figure 3a,b. The energy barriers corresponding to these transition states and the

synchronicities associated with the formation of the corresponding products are reported in Table 4. The results include zero-point energy (ZPE) and counterpoise basis set superposition error (BSSE) corrections. The optimized geometries of the more relevant transition structures for the cycloaddition of **12** and **2a** with pyrrole and 2,5-dimethylpyrrole are presented in Figures 4 and 5, respectively, whereas in Figure 6a, a global picture of the relative barriers for the referred reactions is given. The results demonstrate that the barriers associated with the reactions involving nitrosoalkene **12**, both with pyrrole and dimethylpyrrole, are over 30 kJ/mol higher than those involving **2a**, suggesting that the Diels–Alder reaction is privileged in the case of nitrosoalkene **2a**.

In fact, these results corroborate the experimental findings. The higher energy barriers associated with the transition states involving nitrosoalkene **12** point to a different reaction pathway, as predicted by the experimental results, whereas in the case of the reactions involving nitrosoalkene **2a**, the lower energy barriers are compatible with a process occurring in a concerted way, slightly asynchronous, either with pyrrole and dimethylpyrrole, in both cases through an *endo* approach.

Calculations, at the DFT level, carried out to estimate the relative stability of nitron **18**, with a *cis*-fused ring system, and the corresponding *trans* adduct revealed that the *trans* derivative, which was not detected, would be around 119.2 kJ/mol less stable. On the other hand, calculations also indicate that nitron **18**, with an imine group, is around 40.5 kJ/mol more stable than the tautomeric enamine resulting from a 1,3-hydrogen shift. These results are in agreement with the selective synthesis of nitron **18** from cyclization of intermediate **22** (Scheme 5).

The reaction of nitrosoalkene **2b**,² bearing a 1*H*-tetrazol-5-yl group at C-3, with an excess of 5,5'-diethyldipyrromethane (**8a**) was also studied (Scheme 6). Monofunctionalized dipyrromethane **23** was isolated in 25% yield as the only product. Thus, this synthesis can be best described as being a hetero-Diels–Alder reaction followed by oxazine ring-opening to give the final oxime, the same chemical behavior of nitrosoalkene **2b** observed in the reaction with pyrrole.²

CONCLUSIONS

Herein, new data regarding the chemical behavior of nitrosoalkenes toward dipyrromethanes, pyrrole, and 2,5-dimethylpyrrole has been disclosed. 1-(*p*-Bromophenyl)nitrosoethylene reacts with dipyrromethanes and pyrrole to afford two isomeric oximes via conjugate addition, (*E*)- and (*Z*)-(2'-*p*-bromophenyl-2'-hydroxiiminoethyl)dipyrromethanes and (*E*)- and (*Z*)-(2'-*p*-bromophenyl-2'-hydroxiiminoethyl)pyrrole, respectively. This outcome contrasts with the reactivity observed in the reaction of ethyl nitrosoacrylate with these heterocycles, which leads to (*E*)-oximes as the only products via a Diels–Alder reaction. These nitrosoalkenes also show different reactivity toward 2,5-dimethylpyrrole. Ethyl nitrosoacrylate proceeds via a Diels–Alder reaction to give a bicyclic oxazine, whereas 1-(*p*-bromophenyl)nitrosoethylene undergoes an initial conjugate addition followed by intramolecular O- and N-nucleophilic addition with the formation of the corresponding bicyclic oxazine and five-membered cyclic nitron, respectively.

Quantum chemical calculations, at DFT the level, were carried out to study transition states resulting from the *endo*- and *exo*-cycloadditions of pyrrole and dimethylpyrrole with ethyl nitrosoacrylate and 1-(*p*-bromophenyl)nitrosoethylene. The results indicate that the barriers associated with the Diels–

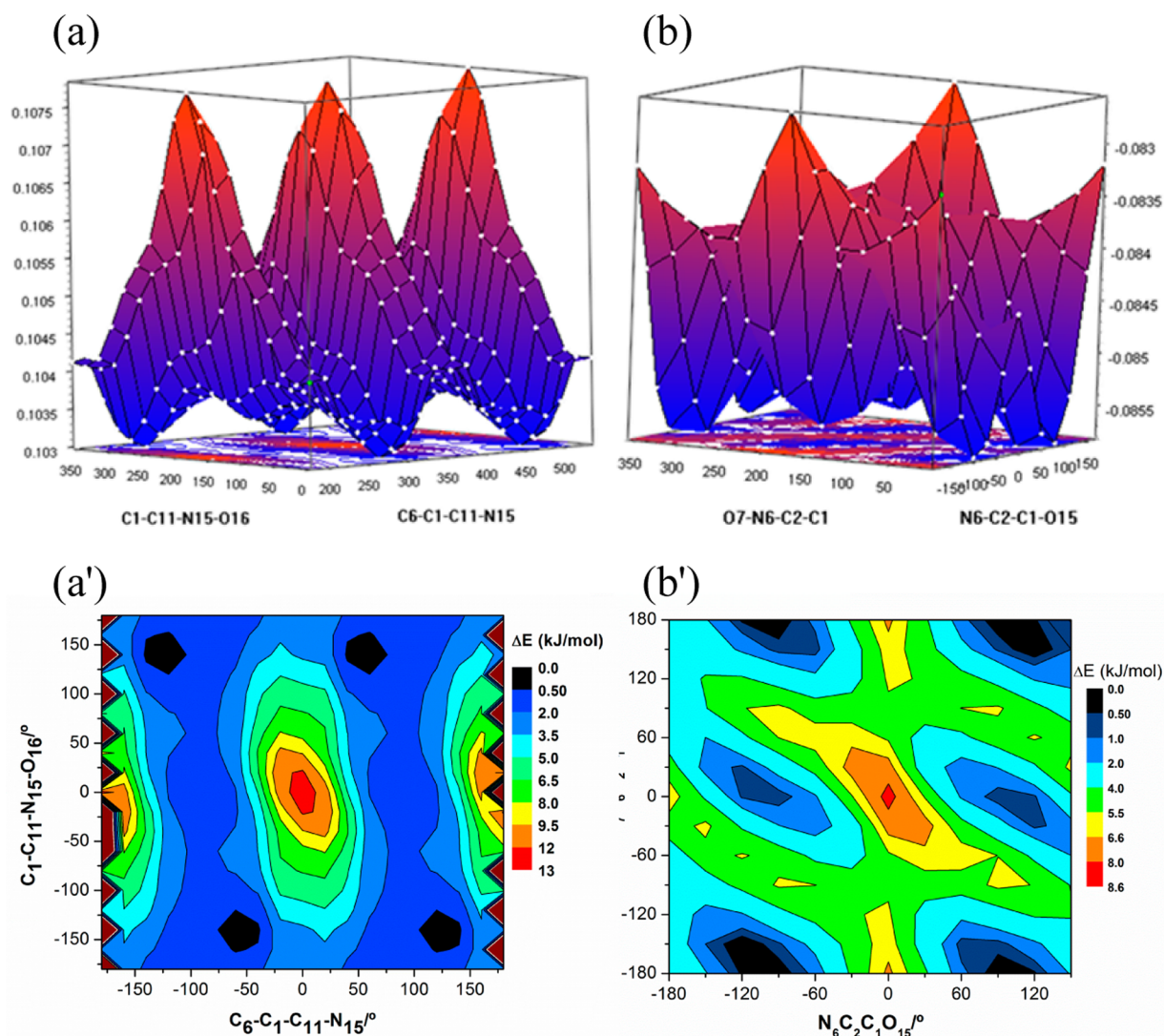


Figure 2. Potential energy profile as a function of the relevant dihedrals (see Figure 1) in compounds **12** (a, a') and **2a** (b, b'), using a step size of 20° and 30° , respectively. At each point, all of the internal coordinates were relaxed (relaxed scan) at the PM3 level. (a', b') Projection of the upper scans in contour form.

Alder reactions of ethyl nitrosoacrylate are over 30 kJ/mol lower than those that would be required for the cycloadditions of 1-(*p*-bromophenyl)nitrosoethylene. Thus, calculations predict that the Diels–Alder reaction is privileged in the case of ethyl nitrosoacrylate and point to a different reaction pathway for 1-(*p*-bromophenyl)nitrosoethylene, corroborating the experimental findings.

EXPERIMENTAL SECTION

General. ^1H NMR spectra were recorded on an instrument operating at 400 MHz. ^{13}C NMR spectra were recorded on an instrument operating at 100 MHz. The solvent was deuteriochloroform unless otherwise indicated. Chemical shifts are expressed in parts per million relative to internal TMS, and coupling constants (J) are in Hz. Infrared spectra (IR) were recorded on a Fourier transform spectrometer. High-resolution mass spectra (HRMS) were obtained on an electrospray (ESI) or electronic impact (EI) TOF mass spectrometer. Melting points were determined in open glass capillaries and are uncorrected. Thin-layer chromatography (TLC) analyses were performed using precoated silica gel plates. Flash column chromatography was performed with silica gel 60 as the stationary phase. 2-Bromo-1-(*p*-bromophenyl)ethanone oxime (**11**),¹⁵ 1-(1-benzyl-1H-

tetrazol-5-yl)-2-bromoethanone oxime (**1b**),² 5,5'-diethyldipyrromethane (**8a**),¹⁶ and 5-phenyldipyrromethane (**8b**)¹⁷ were prepared as described in the literature.

Method A: In Water/Dichloromethane. Dipyrromethanes **8**, pyrrole, or 2,5-dimethylpyrrole (1.08 mmol) and a solution of oximes **1b** or **11** (0.54 mmol) in dichloromethane (1.5 mL) were added to a solution of Na_2CO_3 (2.7 mmol) in water (9 mL). The reaction mixture was stirred at room temperature for 2 h. After this time, the mixture was extracted with dichloromethane (3×20 mL) and dried over Na_2SO_4 , and the solvent was evaporated. The product was purified by flash chromatography.

Method B: In Dichloromethane. Dipyrromethanes **8**, pyrrole, or 2,5-dimethylpyrrole (1.08 mmol) and oximes **1b** or **11** (0.54 mmol) were added to a suspension of Na_2CO_3 (2.7 mmol) in dichloromethane (30 mL). The reaction mixture was stirred at room temperature for the time indicated in each case. The reaction was monitored by TLC. Upon completion, the mixture was filtered through a Celite pad, which was washed with dichloromethane. The solvent was evaporated, and the product was purified by flash chromatography.

(*E*)-1-(2'-*p*-Bromophenyl-2'-hydroxyiminoethyl)-5,5'-diethyldipyrromethane (**13a**) and (*Z*)-1-(2'-*p*-Bromophenyl-2'-hydroxyiminoethyl)-5,5'-diethyldipyrromethane (**14a**). Obtained from oxime **11** (158 mg, 0.54 mmol) and dipyrromethane **8a** (218 mg,

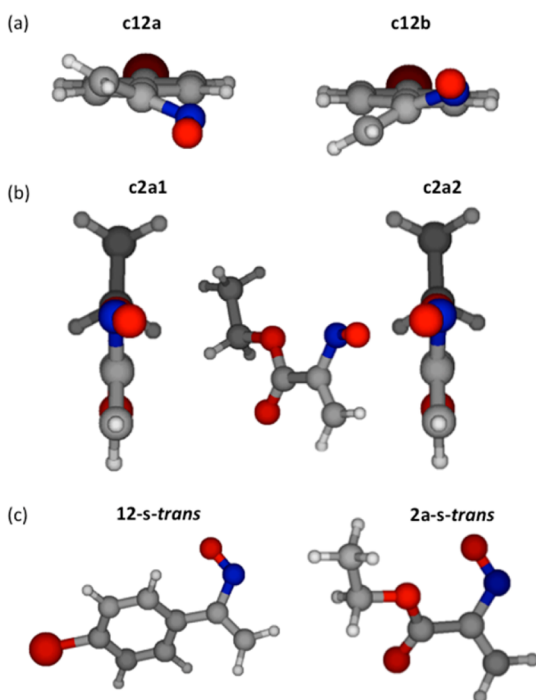


Figure 3. Optimized geometries, at the DFT level, of low energy conformers of nitrosoalkenes **12** (a) and **2a** (b). (c) *Trans*-conformers of both nitrosoalkenes. Color code: gray, carbon; red, oxygen; blue, nitrogen; white, hydrogen; and dark red, bromide.

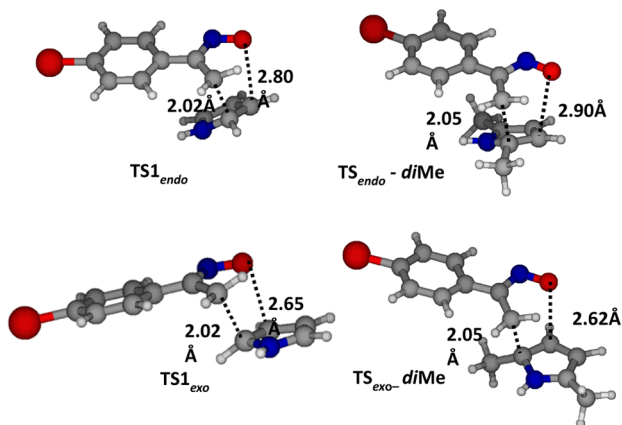


Figure 4. Optimized geometries (B3LYP/6-31G(d,p) level) of the most relevant transition state structures found for the reaction of **12** with pyrrole and 2,5-dimethylpyrrole. Color code: gray refers to carbon, red to oxygen, blue to nitrogen, white to hydrogen, and dark red to bromine atoms.

1.08 mmol) as described in general procedure methods A and B (reaction time, 44 h). Purification of the crude product by flash chromatography (ethyl acetate/hexane, 1:2), gave, in order of elution, **13a** obtained as a white solid (method A: 36 mg, 16%; method B: 102 mg, 46%) and **14a** obtained as a yellow solid (method A: 60 mg, 27%; method B: 80 mg, 36%).

Compound 13a. mp 136.4–137.2 °C (from diethyl ether/hexane). IR (KBr) ν 739, 973, 1489, 2968, 3351, 3423 cm^{-1} . ^1H NMR δ 0.68 (t, $J = 7.2$ Hz, 6H), 1.88 (q, $J = 7.2$ Hz, 4H), 3.92 (s, 2H), 5.89 (d, $J = 2.4$ Hz, 1H), 5.91 (d, $J = 2.8$ Hz, 1H), 6.05 (br s, 1H), 6.09 (d, $J = 2.8$ Hz, 1H), 6.57 (br s, 1H), 7.45–7.50 (m, 4H), 7.75 (br s, 1H), 7.93 (br s, 1H), 8.11 (br s, 1H). ^{13}C NMR δ 8.4, 25.6, 29.5, 43.5, 105.6, 105.7, 106.2, 107.3, 116.7, 123.8, 125.0, 128.0, 131.7, 134.4,

136.4, 136.6, 156.7. HRMS (ESI-TOF): calcd. for $\text{C}_{21}\text{H}_{25}\text{BrN}_3\text{O}$, 414.11755 [$\text{M} + \text{H}^+$]; found, 414.11786.

Compound 14a. mp 117.5–119.0 °C (from diethyl ether/hexane). IR (KBr) ν 785, 1012, 1485, 2965, 3369, 3388 cm^{-1} . ^1H NMR δ 0.64 (t, $J = 7.2$ Hz, 6H), 1.79–1.88 (m, 4H), 3.69 (s, 2H), 5.83 (br s, 1H), 5.94 (br s, 1H), 6.02 (br s, 1H), 6.10 (d, $J = 2.4$ Hz, 1H), 6.54 (br s, 1H), 7.16 (d, $J = 8.4$ Hz, 2H), 7.47 (d, $J = 8.4$ Hz, 2H), 7.62 (br s, 1H), 7.76 (br s, 1H), 8.11 (br s, 1H). ^{13}C NMR δ 8.3, 29.3, 34.1, 43.4, 105.6, 106.4, 107.1, 107.3, 116.8, 123.3, 124.7, 129.5, 131.4, 131.5, 136.72, 136.73, 155.8. HRMS (ESI-TOF): calcd. for $\text{C}_{21}\text{H}_{25}\text{BrN}_3\text{O}$, 414.11755 [$\text{M} + \text{H}^+$]; found, 414.11807.

(E)-1-(2'-p-Bromophenyl-2'-hydroxyiminoethyl)-5-phenyldipyrromethane (13b) and (Z)-1-(2'-p-Bromophenyl-2'-hydroxyiminoethyl)-5-phenyldipyrromethane (14b). Obtained from oxime **11** (158 mg, 0.54 mmol) and dipyrromethane **8b** (240 mg, 1.08 mmol) as described in general procedure methods A and B (reaction time, 24 h). Purification of the crude product by flash chromatography (ethyl acetate/hexane, 1:3), gave, in order of elution, **13b** obtained as a brown solid (method A: 30 mg, 13%; method B: 61 mg, 26%) and **14b** obtained as a brown solid (method A: 63 mg, 27%; method B: 87 mg, 37%).

Compound 13b. mp 99.4–102.0 °C (from diethyl ether/hexane). IR (KBr) ν 725, 1074, 1489, 1587, 1676, 3058, 3414 cm^{-1} . ^1H NMR δ 3.97 (s, 2H), 5.37 (s, 1H), 5.71 (br s, 1H), 5.85 (br s, 1H), 5.94 (br s, 1H), 6.09 (d, $J = 2.8$ Hz, 1H), 6.62 (br s, 1H), 7.15–7.28 (m, 5H), 7.46–7.52 (m, 4H), 7.89 (br s, 1H), 8.36 (br s, 2H). ^{13}C NMR δ 25.7, 44.1, 107.0, 107.1, 107.1, 108.3, 117.1, 123.9, 125.5, 126.9, 128.0, 128.4, 128.6, 131.8, 132.3, 132.6, 134.3, 142.1, 156.7. HRMS (ESI-TOF): calcd. for $\text{C}_{23}\text{H}_{21}\text{BrN}_3\text{O}$, 434.08625 [$\text{M} + \text{H}^+$]; found, 434.08595.

Compound 14b. mp 110.1–112.0 °C (from diethyl ether/hexane). IR (KBr) ν 727, 1010, 1487, 1587, 1676, 3060, 3357, 3408 cm^{-1} . ^1H NMR δ 3.71 (s, 2H), 5.32 (s, 1H), 5.69 (br s, 1H), 5.78 (br s, 1H), 5.83 (br s, 1H), 6.10 (d, $J = 2.4$ Hz, 1H), 6.58 (br s, 1H), 7.10 (d, $J = 7.2$ Hz, 2H), 7.20–7.28 (m, 5H), 7.47 (d, $J = 8.0$ Hz, 2H), 7.86 (s, 1H), 7.91 (s, 1H), 8.26 (br s, 1H). ^{13}C NMR δ 34.1, 44.0, 107.1, 107.8, 107.9, 108.3, 117.3, 123.5, 125.3, 126.9, 128.3, 128.6, 129.6, 131.4, 131.5, 132.5, 132.7, 142.0, 155.7. HRMS (ESI-TOF): calcd. for $\text{C}_{23}\text{H}_{21}\text{BrN}_3\text{O}$, 434.08625 [$\text{M} + \text{H}^+$]; found, 434.08599.

(E)-1-(p-Bromophenyl)-2-(1H-pyrrol-2-yl)ethanone Oxime (15) and (Z)-1-(p-Bromophenyl)-2-(1H-pyrrol-2-yl)ethanone Oxime (16). Obtained from oxime **11** (158 mg, 0.54 mmol) and pyrrole (0.375 mL, 5.4 mmol) as described in general procedure methods A and B (reaction time, 40 h). Purification of the crude product by flash chromatography (ethyl acetate/hexane, 1:3), gave, in order of elution, **15** obtained as a white solid (method A: 42 mg, 28%; method B: 56 mg, 37%) and **16** obtained as a white solid (method A: 66 mg, 44%; method B: 23 mg, 15%).

Compound 15. mp 141.4–142.3 °C (from ethyl acetate/hexane). IR (KBr) ν 717, 910, 1088, 1489, 1585, 3282, 3411 cm^{-1} . ^1H NMR δ 4.09 (s, 2H), 6.05 (br s, 1H), 6.10 (d, $J = 2.8$ Hz, 1H), 6.69 (d, $J = 0.8$ Hz, 1H), 7.50 (d, $J = 8.8$ Hz, 2H), 7.57 (d, $J = 8.4$ Hz, 2H), 8.68 (br s, 2H). ^{13}C NMR δ 25.7, 107.0, 108.1, 117.6, 124.0, 125.9, 128.0, 131.8, 134.2, 157.0. HRMS (ESI-TOF): calcd. for $\text{C}_{12}\text{H}_{12}\text{BrN}_2\text{O}$, 279.01275 [$\text{M} + \text{H}^+$]; found, 279.01248.

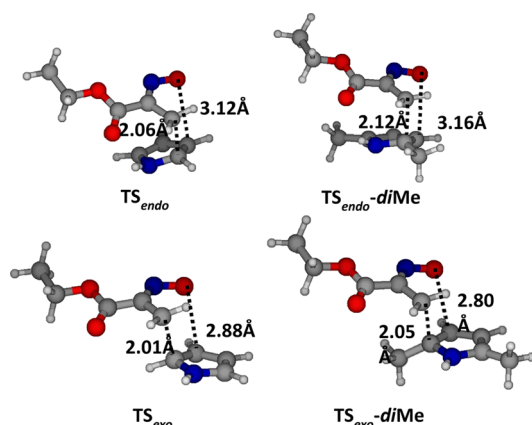
Compound 16. mp 142.1–143.6 °C (from ethyl acetate/hexane). IR (KBr) ν 712, 831, 989, 1078, 1489, 1573, 3184, 3363 cm^{-1} . ^1H NMR δ 3.81 (s, 2H), 5.93 (br s, 1H), 6.10 (d, $J = 2.4$ Hz, 1H), 6.65 (d, $J = 0.8$ Hz, 1H), 7.20 (d, $J = 8.4$ Hz, 2H), 7.49 (d, $J = 8.4$ Hz, 2H), 7.75 (br s, 1H), 8.23 (br s, 1H). ^{13}C NMR δ 34.1, 107.6, 108.7, 117.8, 123.5, 125.7, 129.6, 131.5, 131.6, 155.8. HRMS (ESI-TOF): calcd. for $\text{C}_{12}\text{H}_{12}\text{BrN}_2\text{O}$, 279.01275 [$\text{M} + \text{H}^+$]; found, 279.01247.

3-(p-Bromophenyl)-4a,6-dimethyl-4,4a,7,7a-tetrahydropyrrolo[2,3-e][1,2]oxazine (17) and 2-(p-Bromophenyl)-3a,5-dimethyl-3,3a,6,6a-tetrahydropyrrolo[3,2-b]pyrrole-1-oxide (18). Obtained from oxime **11** (158 mg, 0.54 mmol) and 2,5-dimethylpyrrole (0.549 mL, 5.4 mmol) as described in general procedure methods A and B (reaction time, 6 h). Purification of the crude product by flash chromatography (ethyl acetate/hexane, 2:1 and 5:1; ethyl acetate and ethyl acetate/methanol, 9:1), gave, in order of

Table 4. Energy Barriers, ΔE , and Asynchronicity, *Async*, of the Transition States for the Reaction of **12** and **2a** with Pyrrole and 2,5-Dimethylpyrrole^a

reaction	TS	ΔE (kJ/mol)	d(C–C)/Å	d(O–C)/Å	<i>Async</i>
12 + pyrrole	TS1 _{endo}	66.4	2.02	2.80	0.16
	TS2 _{endo}	66.4	2.02	3.17	0.22
	TS1 _{exo}	72.5	2.02	2.65	0.13
	TS2 _{exo}	72.5	2.02	2.39	0.08
	TS3 _{exo}	72.6	2.02	2.66	0.14
12 + 2,5-dimethylpyrrole	TS _{endo}	60.4	2.05	2.90	0.17
	TS _{exo}	74.1	2.05	2.62	0.12
2a + pyrrole	TS _{endo}	29.1	2.06	3.12	0.20
	TS _{exo}	48.3	2.01	2.88	0.18
2a + 2,5-dimethylpyrrole	TS _{endo}	26.9	2.12	3.16	0.20
	TS _{exo}	49.0	2.05	2.80	0.15

^aCalculated at the B3LYP/6-31G(d,p) level of theory considering the lower energy conformer of each nitrosoalkene. ZPE and BSSE corrections were taken into account. Asynchronicity was calculated according to $Async = [d(C-O) - d(C-C)] / [d(C-O) + d(C-C)]$. Parameters d(C–C) and d(C–O) correspond to the lengths, in the transition state, of carbon–carbon and carbon–oxygen formed bonds, respectively, as indicated in Figures 4 and 5.

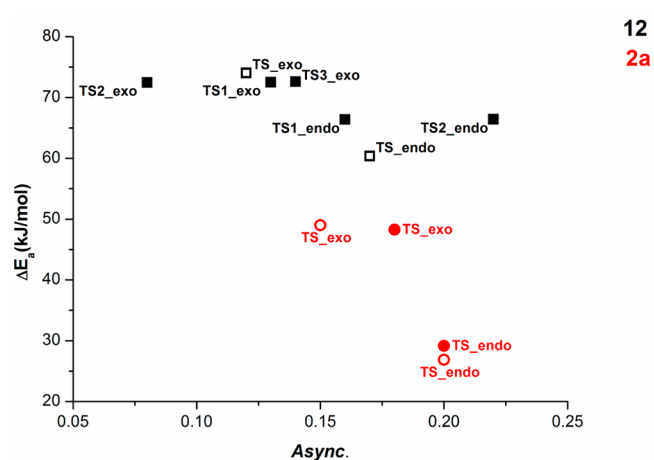
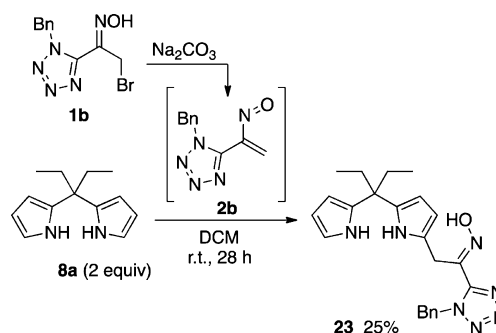
**Figure 5.** Optimized geometries (B3LYP/6-31G(d,p) level) of the transition state structures found for the reaction between **2a** and pyrrole or 2,5-dimethylpyrrole. Color code: gray, carbon; red, oxygen; blue, nitrogen; and white, hydrogen.

elution, **17** obtained as a brown oil (method A: 50 mg, 30%; method B: 71 mg, 43%) and **18** obtained as a yellow solid (method A: 80 mg, 48%; method B: 51 mg, 31%).

Compound 17. IR (film CH₂Cl₂) ν 821, 1008, 1381, 1649 cm⁻¹. ¹H NMR δ 1.27 (s, 3H, H-8), 1.98 (s, 3H, H-9), 2.66 (d, *J* = 14.4 Hz, 1H, H-4), 2.76 (d, *J* = 14.4 Hz, 1H, H-4), 2.81 (d, *J* = 18.8 Hz, 1H, H-7), 2.95 (dd, *J* = 18.8 and 7.2 Hz, 1H, H-7), 4.12 (d, *J* = 6.8 Hz, 1H, H-7a), 7.51 (d, *J* = 8.4 Hz, 2H, H-11 and H-15), 7.55 (d, *J* = 8.4 Hz, 2H, H-12 and H-14). ¹³C NMR δ 19.7 (C-9), 25.9 (C-8), 33.6 (C-4), 45.3 (C-7), 78.8 (C-4a), 83.2 (C-7a), 125.1 (C-13), 127.7 (C-12 and C-14), 132.0 (C-11 and C-15), 133.5 (C-10), 170.0 (C-3), 172.6 (C-6). HRMS (EI-TOF): calcd. for C₁₄H₁₅BrN₂O, 306.0368 [M⁺]; found, 306.0371.

Compound 18. mp 94.5–95.9 °C (from ethyl acetate/hexane). IR (KBr) ν 827, 1220, 1371, 1574, 1645 cm⁻¹. ¹H NMR δ 1.45 (s, 3H), 2.04 (s, 3H), 2.95 (dd, *J* = 18.8 and 7.2 Hz, 1H), 3.18 (d, *J* = 18.0 Hz, 1H), 3.34–3.47 (m, 2H), 4.42 (d, *J* = 7.2 Hz), 7.52 (d, *J* = 8.4 Hz, 2H), 8.21 (d, *J* = 8.4 Hz, 2H). ¹³C NMR δ 19.6, 24.4, 43.0, 43.3, 74.2, 81.8, 124.8, 128.0, 129.2, 131.8, 138.7, 171.7. HRMS (EI-TOF): calcd. for C₁₄H₁₅BrN₂O, 306.0368 [M⁺]; found, 306.0381.

1-[2'-(1''-Benzyl-1H-tetrazol-5-yl)-2'-hydroxyiminoethyl]-5,5'-diethylpiperomethane (23). Obtained from compound **1b** (159 mg, 0.54 mmol) and dipyrromethane **8a** (218 mg, 1.08 mmol) as described in general procedure method B (reaction time, 28 h). After purification by flash chromatography (ethyl acetate/hexane, 1:2 and 1:1), compound **23** was obtained as a beige solid (method B: 47.3 mg,

**Figure 6.** B3LYP/6-31G(d,p) energy (kJ/mol) and asynchronicity, *Async*, of the transition state structures for the reactions: *endo*-(**12** + pyrrole), *exo*-(**12** + pyrrole), *endo*-(**12** + diMe-pyrrole), *exo*-(**12** + diMe-pyrrole), *endo*-(**2a** + pyrrole), *exo*-(**2a** + pyrrole), *endo*-(**2a** + diMe-pyrrole), and *exo*-(**2a** + diMe-pyrrole). Color code: black symbols refer to TS involving nitrosoalkene **12**, while red symbols correspond to TS involving nitrosoalkene **2a**. Filled symbols refer to TS with pyrrole, and empty symbols refer to TS with dimethylpyrrole.**Scheme 6. Hetero-Diels–Alder of Nitrosoalkene **2b** with 5,5'-Diethylpiperomethane (**8a**)**

21%). mp 121.1–122.3 °C (from diethyl ether/hexane). IR (KBr) ν 725, 735, 977, 1068, 1456, 2970, 3365, 3427 cm⁻¹. ¹H NMR (DMSO-*d*₆) δ 0.55 (t, *J* = 6.8 Hz, 6H), 1.89 (pseudo d, *J* = 7.2 Hz, 4H), 4.09 (s, 2H), 5.32 (br s, 1H), 5.58 (br s, 1H), 5.79 (br s, 1H), 5.82 (s, 2H),

5.87 (br s, 1H), 6.55 (br s, 1H), 7.22–7.35 (m, 5H), 9.80 (s, 1H), 10.09 (s, 1H), 12.57 (s, 1H). ^{13}C NMR (DMSO- d_6) δ 8.3, 24.8, 28.2, 42.6, 51.7, 104.5, 104.7, 104.8, 106.2, 116.5, 123.2, 127.8, 128.2, 128.7, 134.7, 136.1, 136.6, 145.2, 150.2. HRMS (ESI-TOF): calcd. for $\text{C}_{23}\text{H}_{28}\text{N}_2\text{O}$, 418.23498 [$\text{M} + \text{H}^+$]; found, 418.23398.

Crystallographic Data for (E)-1-(2'-p-Bromophenyl)-2'-hydroxyiminoethyl)-5,5'-diethyldipyrromethane (13a) and 2-(p-Bromophenyl)-3a,5-dimethyl-3,3a,6,6a-tetrahydropyrrolo[3,2-b]pyrrole-1-oxide (18) X-ray Diffraction. Crystal of compounds 13a and 18 were selected, covered with polyfluoroether oil, and mounted on a nylon loop. Crystallographic data for these compounds were collected at the IST using graphite monochromated Mo $K\alpha$ radiation ($\lambda = 0.71073 \text{ \AA}$) on a diffractometer equipped with an Oxford Cryosystem open-flow nitrogen cryostat, at 150 K. Cell parameters were retrieved and refined on all observed reflections. Absorption corrections were applied using SADABS.¹⁸ Structure solution and refinement were performed using direct methods with the program SIR2004¹⁹ included in the package of programs WINGX-version 1.80.05²⁰ and SHELXL.²¹ All structures refined to a perfect convergence, even though one of the crystals (18) was of poorer quality, which presented high R_{int} and a relatively low ratio of observed/unique reflections. In molecule A of compound 13a, for one of the ethyl moieties, a certain extent of disorder was observed for atom C15, with 53 and 47% probabilities. Non-hydrogen atoms were refined with anisotropic thermal parameters. Except for the NH groups, all hydrogen atoms were inserted in idealized positions and allowed to refine riding on the parent carbon atom with C–H distances of 0.95, 0.98, 0.99, and 1.00 \AA for aromatic, methyl, methylene, and methine H atoms, respectively, and with $U_{\text{iso}}(\text{H}) = 1.2U_{\text{eq}}(\text{C})$ and also on the parent oxygen atom with an O–H distance of 0.84 \AA and with $U_{\text{iso}}(\text{H}) = 1.5U_{\text{eq}}(\text{O})$. Graphic presentations were prepared with ORTEP-III.²²

■ ASSOCIATED CONTENT

■ Supporting Information

^1H and ^{13}C NMR spectra for all new compounds, crystallographic data for compounds 13a and 18, and theoretical calculation results. This material is available free of charge via the Internet at <http://pubs.acs.org>.

■ AUTHOR INFORMATION

■ Corresponding Author

*E-mail: tmelo@ci.uc.pt.

■ Notes

The authors declare no competing financial interest.

■ ACKNOWLEDGMENTS

Thanks are due to Fundação para a Ciência e a Tecnologia (FCT), Portuguese Agency for Scientific Research (Coimbra Chemistry Centre through the project Pest-OE/QUI/UI0313/2014 and Centro de Química Estrutural through the project Pest-OE/QUI/UI0100/2013 and RECI/QEQ-QIN70189/2012) for financial support. Sandra C. C. Nunes, Susana M. M. Lopes, and Clara S. B. Gomes also acknowledge FCT for postdoctoral research grants SFRH/BPD/71683/2010, SFRH/BPD/84413/2012, and SFRH/BPD/64423/2009, respectively. We acknowledge the UC-NMR facility for obtaining the NMR data, which is supported in part by FEDER, European Regional Development Fund through the COMPETE Programme (Operational Programme for Competitiveness) and by National Funds through FCT (Portuguese Foundation for Science and Technology) through grants REEQ/481/QUI/2006, RECI/QEQQFI/0168/2012, CENTRO-07-CT62-FEDER-002012, and Rede Nacional de Ressonância Magnética Nuclear (RNRMN).

■ REFERENCES

- (a) Gilchrist, T. L.; Lemos, A. *J. Chem. Soc., Perkin Trans. 1* **1993**, 1391–1395. (b) Gilchrist, T. L.; Lemos, A. *Tetrahedron* **1992**, *48*, 7655–7662.
- (a) Lopes, S. M. M.; Lemos, A.; Pinho e Melo, T. M. V. D. *Tetrahedron Lett.* **2010**, *51*, 6756–6759. (b) Lopes, S. M. M.; Lemos, A.; Pinho e Melo, T. M. V. D.; Palacios, F. *Tetrahedron* **2011**, *67*, 8902–8909.
- (a) Gilchrist, T. L. *Chem. Soc. Rev.* **1983**, *12*, 53–73. (b) Gilchrist, T. L.; Wood, J. E. In *Comprehensive Heterocyclic Chemistry II*; Boulton, A. J., Ed.; Pergamon Press: Oxford, 1996; Vol. 6, pp 279–299. (c) Lyapkalo, I. M.; Ioffe, S. *Russ. Chem. Rev.* **1998**, *67*, 467–484. (d) Reissig, H.-U.; Zimmer, R. In *1-Nitrosoalkenes*; Molander, G. A., Ed.; Science of Synthesis: Stuttgart, Germany, 2006; Vol. 33, pp 371–389. (e) Sukhorukov, A. Y.; Ioffe, S. L. *Chem. Rev.* **2011**, *111*, 5004–5041.
- (a) Domingo, L. R.; Picher, M. T.; Arroyo, P. *Eur. J. Org. Chem.* **2006**, 2570–2580. (b) Domingo, L. R.; Pérez, P.; Sáez, J. A. *Tetrahedron* **2013**, *69*, 107–114. (c) Domingo, L. R.; Pérez, P.; Sáez, J. A. *RSC Adv.* **2013**, *3*, 1486–1494.
- (a) Gilchrist, T. L.; Stretch, W. J. *J. Chem. Soc., Perkin Trans. 1* **1987**, 2235–2239.
- (a) Gryko, D. T.; Gryko, D.; Lee, C.-H. *Chem. Soc. Rev.* **2012**, *41*, 3780–3789. (b) Lindsey, J. S. *Acc. Chem. Res.* **2010**, *43*, 300–311. (c) Wood, T. E.; Thompson, A. *Chem. Rev.* **2007**, *107*, 1831–1861. (d) Yedukondalu, M.; Ravikanth, M. *Coord. Chem. Rev.* **2011**, *255*, 547–573. (e) Pareek, Y.; Ravikanth, M.; Chandrashekar, T. K. *Acc. Chem. Res.* **2012**, *45*, 1801–1816. (f) Roznyatovskiy, V. V.; Lee, C.-H.; Sessler, J. L. *Chem. Soc. Rev.* **2013**, *42*, 1921–1933. (g) Pereira, N. A. M.; Pinho e Melo, T. M. V. D. *Org. Prep. Proced. Int.* **2014**, *46*, 183–213. (h) Loudet, A.; Burgess, K. *Chem. Rev.* **2007**, *107*, 4891–4932. (i) Ulrich, G.; Ziesel, R.; Harriman, A. *Angew. Chem., Int. Ed.* **2008**, *47*, 1184–1201. (j) Benstead, M.; Mehl, G. H.; Boyle, R. W. *Tetrahedron* **2011**, *67*, 3573–3601. (k) Boens, N.; Leen, V.; Dehaen, W. *Chem. Soc. Rev.* **2012**, *41*, 1130–1172. (l) Beer, P. D.; Gale, P. A. *Angew. Chem., Int. Ed.* **2001**, *40*, 486–516. (m) Caltagirone, C.; Gale, P. A. *Chem. Soc. Rev.* **2009**, *38*, 520–563. (n) Wenzel, M.; Hiscock, J. R.; Gale, P. A. *Chem. Soc. Rev.* **2012**, *41*, 480–520.
- (a) Pereira, N. A. M.; Lemos, A.; Serra, A. C.; Pinho e Melo, T. M. V. D. *Tetrahedron Lett.* **2013**, *54*, 1553–1557. (b) Lopes, S. M. M.; Lemos, A.; Pinho e Melo, T. M. V. D. *Eur. J. Org. Chem.* **2014**, in press.
- Pereira, N. A. M.; Lopes, S. M. M.; Lemos, A.; Pinho e Melo, T. M. V. D. *Synlett* **2014**, *25*, 423–427.
- Allen, F. H. *Acta Crystallogr., Sect. B: Struct. Sci.* **2002**, *58*, 380–388.
- (a) Tiecco, M.; Testaferri, L.; Tingoli, M.; Bagnoli, L.; Marini, F. *J. Chem. Soc., Perkin Trans. 1* **1993**, 1989–1993. (b) Grigg, R.; Hadjisoteriou, M.; Kennewell, P.; Markandu, J. *J. Chem. Soc., Chem. Commun.* **1992**, 1537–1538. (c) Grigg, R.; Hadjisoteriou, M.; Kennewell, P.; Markandu, J.; Thornton-Pett, M. *J. Chem. Soc., Chem. Commun.* **1993**, 1340–1342. (d) Bowman, W. R.; Davies, R. V.; Slawin, M. Z.; Sohal, G. S.; Titman, R. B.; Wilkins, D. J. *J. Chem. Soc., Perkin Trans. 1* **1997**, 155–161. (e) Tiecco, M.; Testaferri, L.; Bagnoli, L.; Purgatorio, V.; Temperini, A.; Marini, F.; Santi, C. *Tetrahedron: Asymmetry* **2001**, *12*, 3297–3304. (f) Dondas, H. A.; Grigg, R.; Hadjisoteriou, M.; Markandu, J.; Kennewell, P.; Thornton-Pett, M. *Tetrahedron* **2001**, *57*, 1119–1128.
- (a) Davies, D.; Gilchrist, T. L.; Roberts, T. G. *J. Chem. Soc., Perkin Trans. 1* **1983**, 1275–1281.
- Frisch, M. J.; Trucks, G. W.; Schlegel, H. B.; Scuseria, G.; Robb, M. A.; Cheeseman, J. R.; Montgomery Jr., J. A.; Vreven, T.; Kudin, K. N.; Burant, J. C.; Millam, J. M.; Iyengar, S. S.; Tomasi, J.; Barone, V.; Mennucci, B.; Cossi, M.; Scalmani, G.; Rega, N.; Petersson, G. A.; Nakatsuji, H.; Hada, M.; Ehara, M.; Toyota, K.; Fukuda, R.; Hasegawa, J.; Ishida, M.; Nakajima, T.; Honda, Y.; Kitao, O.; Nakai, H.; Klene, M.; Li, X.; Knox, J. E.; Hratchian, H. P.; Cross, J. B.; Bakken, V.; Adamo, C.; Jaramillo, J.; Gomperts, R.; Stratmann, R. E.; Yazyev, O.; Austin, A. J.; Cammi, R.; Pomelli, C.; Ochterski, J. W.; Ayala, P. Y.; Morokuma, K.; Voth, G. A.; Salvador, P.; Dannenberg, J. J.

Zakrzewski, V. G.; Dapprich, S.; Daniels, A. D.; Strain, M. C.; Farkas, O.; Malick, D. K.; Rabuck, A. D.; Raghavachari, K.; Foresman, J. B.; Ortiz, J. V.; Cui, Q.; Baboul, A. G.; Clifford, S.; Cioslowski, J.; Stefanov, B. B.; Liu, G.; Liashenko, A.; Piskorz, P.; Komaromi, I.; Martin, R. L.; Fox, D. J.; Keith, T.; Al-Laham, M. A.; Peng, C. Y.; Nanayakkara, A.; Challacombe, M.; Gill, P. M. W.; Johnson, B.; Chen, W.; Wong, M. W.; Gonzalez, C.; Pople, J. A. *Gaussian 03*, revision D.01; Gaussian, Inc.: Wallingford, CT, 2004.

(13) Schmidt, M. W.; Baldridge, K. K.; Boatz, J. A.; Elbert, S. T.; Gordon, M. S.; Jensen, J. H.; Koseki, S.; Matsunaga, N.; Nguyen, K. A.; Su, S. J.; Windus, T. L.; Dupuis, M.; Montgomery, J. A. *J. Comput. Chem.* **1993**, *14*, 1347–1363.

(14) (a) Becke, A. D. *Phys. Rev. A* **1988**, *38*, 3098–3100. (b) Becke, A. D. *J. Chem. Phys.* **1993**, *98*, 5648–5652. (c) Lee, C. T.; Yang, W. T.; Parr, R. G. *Phys. Rev. B* **1988**, *37*, 785–789.

(15) Hartung, J.; Schwarz, M. *Org. Synth.* **2002**, *79*, 228–232.

(16) Sobral, A. J. F. N.; Rebanda, N. G. C. L.; Silva, M.; Lampreia, S. H.; Ramos Silva, M.; Matos Beja, A.; Paixão, J. A.; Gonsalves, A. M. d. R. *Tetrahedron Lett.* **2003**, *44*, 3971–3973.

(17) Littler, B. J.; Miller, M. A.; Hung, C.-H.; Wagner, R. W.; O'Shea, D. F.; Boyle, P. D.; Lindsey, J. S. *J. Org. Chem.* **1999**, *64*, 1391–1396.

(18) Sheldrick, G. M. *SADABS, Program for Empirical Absorption Correction*; University of Göttingen: Göttingen, Germany, 1996.

(19) Burla, M. C.; Caliandro, R.; Camalli, M.; Carrozzini, B.; Cascarano, G. L.; De Caro, L.; Giacovazzo, C.; Polidori, G.; Spagna, R. *J. Appl. Crystallogr.* **2005**, *38*, 381–388.

(20) Farrugia, L. J. *J. Appl. Crystallogr.* **1999**, *32*, 837–838.

(21) (a) Sheldrick, G. M., *SHELX97—Programs for Crystal Structure Analysis*, release 97-2; Institut für Anorganische Chemie der Universität: Göttingen, Germany, 1998. (b) Sheldrick, G. M. *Acta Crystallogr.* **2008**, *A64*, 112–122.

(22) Farrugia, L. J. *J. Appl. Crystallogr.* **1997**, *30*, 565.